CB-Note 280

Split–off Recognition in Data with charged Tracks
The TAXI Logics

M. Benayoun, N. Djaoshvili, P. Hidas, J. Kisiel,
R. Landua, L. Montanet, R. Ouared

CERN, Geneva

June 24, 1995

Abstract : We present a logics named TAXI which aims to remove hadronic split–offs from calorimeter data for $p\bar{p}$ annihilations with charged hadrons in the final state. We present a comparison of data with Monte Carlo simulations which allows to conclude that hadronic showers are better accounted for using FLUKA than GEISHA. We show that the probability of hadronic split–offs is of about 14% per track. We illustrate the working of the criteria we suggest, using annihilations into $\pi^+\pi^-\gamma\gamma\gamma$ data.

1 Introduction

One of the main problems when studying $p\bar{p}$ annihilations in the Crystal Barrel Detector is the recognition and the reconstruction of photons from the information carried by the crystals of the calorimeter. The algorithms allowing recognition of crystal clusters and the way to split them into PEDs (Particle Energy Deposits) released by each charged or neutral (photon) particle are already working tools. Thus an efficient software is already available which allows to reconstruct the energy of the photon and its direction.

The problem which remains is the regognition of split–offs which mimic unduely photons. Split–offs are showers produced by secondary interactions with the calorimeter material at some distance of the particle impact in the calorimeter where the main shower normally expends. These split–offs follow from the stochastic nature of the showers produced by particles (charged or photons) in the crystals of the calorimeter. Thus, there exist two kinds of split–offs (electromagnetic or hadronic) which exhibit different features. Some logics already exist[1, 2, 3] which are well adapted to the recognition of electromagnetic split–offs (SMART, Dolby–C). At Crystal Barrel, there is only one specific study of hadronic split–offs[4] with a highly pessimistic conclusion concerning their possible identification. To remove hadronic split–offs, the most appropriate procedure is the one followed by the CBDROP[5] package, which allows to retain a n–PED configuration as a m–photon event ($m < n$, with $n - m$ fixed by the user) relying on its probability. Its main tool is the energy–momentum conservation. This however does not imply that the rejected configurations have bad probabilities ; more precisely, there exist several configurations where it is not actually possible to distinguish reliably a split–off from a real energy photon. In order to lower the efficiency threshold of the calorimeter, any method allowing to remove beforehand some PEDs from an event is desirable.

The present note aims to present a method, named TAXI, to remove hadronic split–offs on purely topological grounds. The method is based on a new clustering algorithm which follows from the specific properties of hadronic clusters and split–offs observed in collinear events ($p\bar{p} \rightarrow \pi^+\pi^-$) ; all this is the subject of section 2 and 3, where we show how to choose the most sensitive among the threshold parameters. Having chosen the most likely threshold values, we study the shower probabilities in hadronic events in section 4.

In section 5 we show that the shower simulation FLUKA is in better agreement with the data than GEISHA. In section 6, we list the set of conditions for an efficient removal of hadronic

split–offs. Section 7 is devoted to illustrate on real events the effect of the proposed cuts.

2 Clusters in Photon and Hadron Showers

The Crystal Barrel Calorimeter is segmented into 1380 individual CsI crystals. Any pattern recognition method used on data provided by this kind of calorimeter supposes first to define the minimum energy value (the so–called EXTLBC parameter in BCTRAK software) above which the energy provided by a crystal is considered significant, second a clustering algorithm. The step further is to subdivide the cluster into PEDs following an algorithm already implemented in BCTRAK. Each PED is supposed to be associated with a particle hitting the calorimeter, photon or hadron. They are built starting from the local maxima inside the clusters.

2.1 The Standard Clustering Algorithm

To explain the working of clustering algorithms, it is easier to figure the barrel as a cylinder, the – inner – surface of which being segmented into 'squares' of equal sides[1].

In order to work out the cluster building, one first needs to define the neighborhood of any crystal. The working algorithm of BCTRAK chooses a topology represented in figure 1 (locally, we can represent the cylinder as a plane) : for a given crystal (shown in black in figure 1), all crystals (shown in shaded) having a corner or a side in common with it belong to its neighborhood. Therefore each crystal has 8 neighbors.

In order to build up clusters, BCTRAK starts from a hit crystal (*i.e.* carrying an energy above a given energy threshold EXTSBC) at some location ($\theta = i$, $\phi = \alpha$). If k among the eight neighbors shown in figure 1 are also hit (*i.e.* they carry an energy above another given threshold EXTLBC already defined) then they are merged with the previous crystal into the same cluster. One then looks the eight neighbors of each newcomer in the cluster and merge the corresponding hit crystals (if above EXTLBC) to the cluster. The procedure stops when all neighbors of any crystal of the cluster are already within the cluster.

Presently the usual values for EXTLBC and EXTSBC are respectively 1 MeV and 4 MeV. EXTSBC is nothing but the threshold energy for the highest energy crystal in a cluster (the so–called Central Crystal). One could also start a cluster from any crystal above EXTLBC and check at the end that the cluster contains at least one crystal carrying an energy above EXTSBC, the final result would be identical. Any cluster carrying an energy smaller than another threshold (ECLUBC) is wiped out ; the default value for this parameter is 20 MeV, however 4 MeV or 10 MeV have also been used to carry on physics analyses.

Another parameter is used by BCTRAK in order to go from clusters to PEDs, EPEDBC. The splitting up of clusters into PEDs is organized around the local maxima of the cluster and a

[1] Actually, the 'squares' in the central 20 rows have angular apertures of 6° in θ (polar angle) and 6° in ϕ (azimuthal angle), the two external sets of three rows have the same θ opening, while in ϕ their opening angle is 12°. For clarity reasons, we shall specialize our discussion to the central part of the calorimeter, simply quoting that the TAXI logics takes into account suitably the external rows.

PED is kept as such if its energy is larger than EPEDBC. Its default value is 20 MeV, however 10 MeV has also been used. This set of parameters is stored in the common block /BCCUTS/.

2.2 Photon and Hadron Showers

The topology described by figure 1 is not unique. However it is well adapted to describe photon showers, as photon showers are expected to expend symmetrically around the photon line of flight. The energy released is also supposed to be maximum on the crystal which intersects the line of flight and to decrease smoothly when moving away from here. The splitting up of clusters into PEDs relies on this property : two local maxima inside the same cluster should correspond to two photons with a small angular opening. However, taking into account the existence of fluctuations in the expending of electromagnetic showers, such a situation could also correspond to a single photon shower and a split–off which has to be added to the main shower. In this case however, the two local maxima have a relatively large energy difference[1].

In the case of hadron showers, the situation is different. Indeed, fluctuations can be much larger for hadronic showers than for electromagnetic showers. The best way to get a feeling of the problem is to study collinear events in annihilations at rest, *i.e.* $p\bar{p} \rightarrow \pi^+\pi^-$ and $p\bar{p} \rightarrow K^+K^-$. These events can be easily identified from JDC data only, as the two tracks emerging from the interaction have trajectories laying on the same circle ; moreover these tracks are monoenergetic (928 MeV for pions, 798 MeV for kaons).

Having a sample of collinear events with nearly no background (≤ 1 to 2 %), we have plotted the full barrel information in order to look what is the hit crystal topology. This topology is highly cut dependent. Assuming a likely set of calorimeter cuts, events with only two clusters matching the two charged tracks are found to represent about a half of the sample. One also finds events with only one cluster, or with two clusters but only one matched cluster ; this category of events are at the percent level. In the second half of the sample, there is always one or more additional clusters. Figure 2 shows such an event with a parasitic cluster located far from the two matched clusters ; even by eyes, it is impossible to attribute unambiguously this split–off to a definite parent cluster. The leftmost cluster clearly illustrates that the expending of the hadronic shower is not symmetric and that the energy released is not mononotically decreasing from the impact to the outermost crystals of the cluster. Scanning of events shows that hadronic cluster topologies are especially rich, in length or shape with maxima randomly spread onto the whole cluster length. They also illustrate that single crystal clusters appear randomly distributed onto the whole barrel, not necessarily close to clusters matching the parent charged tracks. Thus, hadronic showers have very specific features with respect to electromagnetic showers.

First of all, if the concept of PED is physically meaningful when dealing with photons, it is clearly meaningless when dealing with hadrons showers. In collinear events, most hadronic clusters give rise to several PEDs. This calls for caution in the general case of events with photons and hadrons.

A second property is that shower fluctuations can produce an empty gap inside a shower ;

this property has to be accounted for in a clustering algorithm especially devoted to hadron showers. In other words, the clustering algorithm should allow to merge nearby split–offs to the main cluster.

A third topological property is that hadronic split–offs can be randomly distributed onto the whole barrel. They can carry arbitrary energies (possibly larger than the energy of a main – matched – cluster). One can also observe a large number of these split–offs are single crystal clusters which can carry energies from some MeVs up to several hundred MeVs. Of course, if one lowers the threshold values, the mean number of split–offs per event becomes larger and larger. Appropriate threshold energies are an essential tool in dealing with calorimeter data.

Finally, the previous remark concerning the possible existence of several PEDs of arbitrary energy inside a single hadronic cluster sets a twofold problem : i/ How to recognize a fluctuation in an hadronic shower giving a local maximum and a PED produced by a photon ? ii/ Assuming even that a photon shower superimposes to a marginal PED of an hadronic cluster (*i.e.* a PED which does not match geometrically a charged track), how to disantangle the two components in order to extract with a known accuracy the photon energy ?

Question i could be possibly answered provided the PED energy is large enough to influence energy–momentum conservation. We have not found a satisfactory answer to question ii. Taking into account all uncertainties, it looks *a priori* safer to treat hadron clusters globally and accept to loose these PEDs as identified photons. This results in a loss of acceptance on an event by event basis which can be estimated using a Monte Carlo.

2.3 The TAXI Clustering Algorithm

The properties of hadron showers revealed by dozens of barrel plots have been listed just above. They call for another cluster finding algorithm which takes into account the specific features of hadronic showers with respect to photon showers.

The basic idea is to define the neighborhood of a crystal in a way different from the one illustrated in figure 1. We thus define the neighborhood of a crystal α by attributing to it all crystals which are at a taxiblock distance $\leq k$ (k being an integer) from α. Using $k = 1$ (see figure 3a), the neighborhood of a (black) crystal contains 4 (shaded) crystals ; assuming $k = 2$ (see figure 3b), the neighborhood of a (black) crystal is constituted by 12 (shaded) crystals, while $k = 3$ provides a neighborhood of 24 crystals (see figure 3c).

It is interesting to describe the effects of such a definition of a neighborhood on crystal configurations. The working of the algorithm in the present case can be done generally following the way we described above (see section 2.1). Let us only discuss specific examples. For instance, in figure 4a, one finds two clusters if $k = 1$ or only one if $k \geq 2$; figure 4b shows a case where the number of clusters is 3 ($k = 1$) or 1 ($k \geq 2$). The standard clustering algorithm finds one cluster in case of figure 4a and 2 for figure 4b.

Clearly, using a taxiblock distance $k = 2$ allows to have empty gaps of a one crystal width inside a cluster ; if $k = 3$, the empty gap can be of one or two crystal width. The size of the gap obviously increases with k.

Using a taxiblock distance $k \geq 2$ plays nearly as the standard clustering algorithm *plus* an angle condition to merge nearby clusters ; it would play exactly instead of nearly if the barrel were a sphere. Defining a taxiblock distance looks however more natural than an angle condition, as the angle privileges the interaction point for a phenomenon following from a particle reinteraction in the calorimeter.

The precise value to use for k has to be checked on data. Clearly $k = 1$ gives surely too small a neighborhood ; using $k = 4$ begins to allow a cluster to eat nearby clusters up to an angular distance of 18° ; it could render inefficient too large regions of the calorimeter for photon detection.

We have studied hadronic clusters distributions and properties using $k = 2$, 3. It appears that a maximum taxiblock distance $k = 2$ gives already results close to optimum. More precisely, the (hadronic) split–off probabilities are found nearly unchanged when going from $k = 2$ to $k = 3$. Therefore, the TAXI logics just described has to be understood from now on as using a (maximum) taxiblock distance $k = 2$.

3 Parameter Calibration

As recalled in section 2.1, the treatment of the calorimeter information depends on essentially four threshold parameters. Obviously, whichever is the algorithm used to perform pattern recognition in the barrel, the number of clusters in an event depends on the parameter values. Roughly speaking, if all thresholds are put at zero one could find dozen of clusters in collinear events, while pushing all thresholds at large values, we can end up with no information at all in the calorimeter. Therefore, a tuning of the calorimeter parameters has to be performed.

Collinear events provide an appropriate sample for calibration purposes. Using a given sample of collinear events we choose as criterium the evolution of the number n of 2–cluster events as a function of each parameter X. Basically, for too low values of X, the number of 2–cluster events n should be around zero ; rising the value of X, we expect first a rise of n and after some time a fall–off down to zero from some parameter value upwards. In order that a calibration would be meaningful, after a more or less sharp rise, n should reach a plateau. A likely value for the parameter X is a point located slightly after the beginning of the plateau ; clearly, it cannot have a value smaller than the point where the rise of the curve turns to the plateau otherwise the normalization would be too much sensitive to energy fluctuations. Moreover, this behaviour has to be alike in real data and in the Monte Carlo, otherwise all corrections would be questionable.

The most basic parameter is EXTLBC, the minimum energy above which the information carried by crystals is considered as significant. We have fixed it at its default value 1 MeV. Changing this value, would imply to recalibrate also all ADCs ; it happens that this is not necessary.

There are two other parameters which affect the definition of a cluster : EXTSBC – the minimum energy carried by the highest energy crystal in the cluster (*i.e.* the so–called central

crystal) – and ECLUBC – the minimum energy carried by a cluster in order to keep it.

The criterium described above has been studied as a function of the threshold values EXTSBC and ECLUBC. Using a sample of 800 collinear $\pi^+\pi^-$ events, we have drawn the curve giving for each threshold value the number n of 2-cluster events with both cluster energies above this threshold value. Figure 5 shows the result. As a function of ECLUBC (upmost figure) n is a monotonically increasing function upon the whole range explored (from 1 to 20 MeV) ; instead, as a function of EXTSBC – *i.e.* the central crystal energy threshold – n starts to reach a plateau at 8 MeV, and remains nearly constant in the whole explored range (see figure 5 downmost).

These curves allow already two conclusions : i/ The minimum central crystal energy of a cluster (EXTSBC) is a relevant quantity and can be tuned with a nice accuracy ; experimentally this value cannot be chosen below 8 MeV. In order to be less sensitive to fluctuations which could render the normalization unstable, it is appropriate to choose EXTSBC=10 MeV. Indeed a 2 MeV fluctuation on the energy of the central crystal (which can easily be of the order 100 MeV) would result in an error in the normalization of 30% if EXTSBC is chosen too small. It is also clear from the figure that a threshold value EXTSBC=4 MeV – the default value – is by far too small. ii/ There is no sensitivity of our criterium to the threshold energy ECLUBC of the clusters. Using the conclusion i, we can only assert that ECLUBC should be greater than $\simeq 10$ MeV for obvious reasons.

4 Hadronic Split–off Probabilities

We have studied the distribution giving the number of showers per event in a sample of 800 collinear $\pi^+\pi^-$ events[2]. To perform the clustering of hit crystals, we have set the minimum crystal energy (EXTLBC) at 1 MeV and the minimum energy of the central crystal in a cluster (EXTSBC) at 8 MeV ; otherwise stated, we have removed all crystals below 1 MeV and all clusters having a central crystal energy below 8 MeV. Clusters have been constructed using the previously defined TAXI clustering algorithm. The definition used for the neighborhood of a crystal is the taxiblock distance 2 as shown in figure 3b.

The distribution of the number of showers per event is shown in figure 6. We can see here that there is some events with only one cluster ; this illustrates the fact that a charged particle of 900 MeV does not produce necessarily a shower above the energy thresholds in the Crystal Barrel calorimeter. There is still also some events with 10 or 12 showers.

Let us define ϵ_i the probability that one pion produces i showers ($i = 0, 1, 2 \ldots$). ϵ_i is close to the probability that one pion produces $i-1$ split–offs besides the main (matched) cluster[3].

Knowing the entries in each bin of the histogram in figure 6, we can compute the observed probability (more precisely the frequency) P_j to have j showers ($j = 0, 1, 2 \ldots$) above all thresholds in a collinear event. P_j and ϵ_i are related by :

[2]We have also done the same study with collinear K^+K^- events ; the conclusions are essentially the same as for $\pi^+\pi^-$ events.

[3]Indeed the probability, having a cluster, that it matches the charged track is not 100%. Otherwise stated, the interaction of a charged track with the calorimeter can result in only a split–off.

$$\begin{cases} P_0 &= \epsilon_0^2 \\ P_1 &= 2\epsilon_0\epsilon_1 \\ P_2 &= 2\epsilon_0\epsilon_2 + \epsilon_1^2 \\ P_3 &= 2\epsilon_0\epsilon_3 + 2\epsilon_2\epsilon_1 \\ \dots \end{cases} \quad (1)$$

This is a rough statistical model ; for instance, it neglects correlations in the expension of showers associated with each track. It also neglects the probability of having overlapping clusters. Nevertheless it allows to account for the distribution shown in figure 6 up to 7 clusters. In this case, we have :

$$\epsilon_0 + \dots + \epsilon_4 = 1 \ , \ (\epsilon_j = 0, \ j \geq 5) \quad (2)$$

Using the data represented in figure 6, this oversimplified model gives :

$$\begin{cases} \epsilon_1 &= 0.87 \pm 0.01 \\ \epsilon_2 &= 0.11 \pm 0.02 \\ \epsilon_3 &= 0.02 \pm 0.01 \\ \epsilon_4 &= 0.01 \pm 0.01 \end{cases} \quad (3)$$

with a good fit probability ($\chi^2/dof = 0.95/1$). Therefore, using the threshold values given at the beginning of this section and the TAXI cluster algorithm, the total probability to get split–offs is of the order 15% per track. This value is dominated by the probability to get one split–off only ($\simeq 11\%$) per track. This probability for hadronic split–offs is of the same order than the probability to get electromagnetic split–offs in 0–prong events. Moreover, it should be noticed that about a half of the surviving split–offs are single crystal clusters.

5 Monte Carlo Studies

These criteria and several other topics have been studied on Monte Carlo collinear events. Two shower simulations were studied, GEISHA and FLUKA in order to see how they compare with real data in the hadronic sector. Figure 7 shows the energy of the clusters matching the pions found using these Monte Carlo and the data. The minimum ionizing peak is found at the expected place by both GEISHA and FLUKA. However the bump which describes the pion reinteraction inside the calorimeter is much better accounted for by FLUKA than GEISHA.

GEISHA produces too much split–offs for low energy released by hadrons with respect to the data. Figure 8 shows the number of split–offs as a function of the total energy carried by the matched clusters ; it illustrates that the spectrum of GEISHA split–offs is shifted toward low matched energies with respect to the data. FLUKA (not shown) gives a much better agreement.

Another feature which makes FLUKA more appropriate with respect to our data is the curve giving the number n of 2–cluster events in a sample of collinear events as a function of the

minimum energy for central crystal. In this case, FLUKA provides the same plateau effect than the data (see downmost figures 5 and 9) ; however the starting point of this plateau is rather at 13 MeV (instead of 8 MeV in the experimental sample). It is also interesting to remark that the percentage of 2–cluster events at the plateau is 71% with FLUKA and 69 % in the data. Instead, GEISHA does not exhibit any plateau effect.

Comparing FLUKA and GEISHA thus leads us to conclude that our data are in agreement with FLUKA while basic features of are not reproduced by GEISHA. Moreover, in any case where our data have to be normalized to Monte carlo samples, it is better to increase the cut on PEDs by asking the minimum energy of the central crystal to be larger than 13 MeV ; for smaller values the normalization by the Monte Carlo cannot be fully trusted.

Both Monte Carlo and the data exhibit a common feature. There exist a large number of single crystal clusters of generally low energy, typically below 10 MeV. They survive any clustering algorithm including TAXI. In collinear events, after cutting out the full matched clusters reconstructed using TAXI, and all other PEDs having a central crystal energy below $\simeq$ 10 MeV, they still represent about 1/3 of the surviving split-offs. It is therefore useful to cut them out.

However, outside hadronic clusters, the basic quantities are PEDs. A criterium requiring the cluster size to be larger than one, for instance, could therefore bias the data samples. A criterium which has the same effect on small clusters and on PEDs is a cut on the so-called E1/E9 variable. E1/E9 is the ratio of the energy carried by central crystal in the PED to the energy carried by it and the 8 surrounding crystals. In figure 10, we show its distribution in a data sample of collinear events generated with FLUKA. The peak around 1 has clearly to be removed.

6 Split–off Removal

In a standard annihilation event, what can be clearly attributed to charge tracks are the so–called matched clusters, *i.e.* the clusters which intersect the charged track trajectories as reconstructed using the JDC information. All split–offs which can be recognized as such when dealing with collinear events, are mixed with real photon clusters in all other kind of events. Therefore, it is useful to identify other properties of hadronic split–offs in order to remove them and help the kinematical fit.

The first condition is to cut out the whole hadronic matched clusters reconstructed with the TAXI algorithm. In collinear events, the mean number of PEDs in an hadronic cluster is around 4. If we remove only the matched PEDs, we should have to deal further on with several split–offs per event with charge tracks. However, removing the whole hadronic cluster, we also remove at the meantime from analysis events with photons giving showers inside hadronic clusters. On the other hand, because of the specific structure of hadronic showers, such PEDs would have their energy affected in an unpredictable way by the underlying hadronic shower. Removing

globally such photons results in a lost of acceptance which can be accounted for using Monte Carlo generated events having the physics topology under study.

The second condition is to require any other cluster to have a central crystal energy above 8 MeV (EXTSBC). This condition moreover is needed in order to avoid a too large sensitivity to energy fluctuations in hadronic shower structure. In order to match the properties of FLUKA, it is even better to push this threshold up to 13 MeV.

Among hadronic split–offs surviving these two conditions, a large fraction are clusters containing a small number of crystals, typically one, frequently of low energy. These clusters of small size cannot be disantangled from small energy ($\leq$ 10 MeV) photons and electromagnetic splitt-offs. A criterium which looks less sensitive to bias is to remove also all PEDs which have a too large value of E1/E9 ; a suitable cut to accept a PED is E1/E9 $\leq$ 0.96. In figure 11 we show the number of split–offs outside the matched hadronic clusters for collinear events generated using FLUKA. We also show the PED distribution for generated single photons. Clearly the proposed cut on E1/E9 removes an important fraction of hadronic split–offs. Moreover, half of the 2–PED events obtained with generated single photon events carries a large value of E1/E9. Therefore requiring, in order to keep a PED, that its value for E1/E9 should be less than 0.96 removes a large fraction of split–offs, hadronic or electromagnetic as well.

7 Split–off Removal in $\pi^+\pi^-\gamma\gamma\gamma$ Events

It is useful to illustrate on real spectra the effects of the cuts suggested just above. For this purpose, we have used 2–prong data (annihilations at rest, june 91) and looked at the channel with three unmatched PEDs. In this case, the 3 photon mass spectrum can only exhibit the $\rho^0/\omega \rightarrow \pi^0/\eta \ \ \gamma$ signals.

In figure 12 (upmost) we show the 3 γ invariant mass spectrum obtained after only removing electromagnetic split–offs using Dolby–C. The structure between 700 and 800 MeV should be clearly attributed to ρ^0/ω ; the structure around 200 MeV is produced by the merging of a real π^0 with a split–off surviving Dolby–C. Figure 12 (middle) shows the effect produced by removing the whole hadronic clusters reconstructed using the TAXI algorithm and Dolby–C. Finally figure 12 (downmost) shows the result obtained by requiring, in addition to the two previous conditions, the removal of all PEDs having a central crystal energy smaller than 10 MeV and/or E1/E9 $\geq$ 0.96.

Clearly, the removal of the whole hadronic clusters allows to reduce the background by $\simeq$ 30% without affecting physics signals. However the two additional criteria already mentioned allow also for a large additional background suppression. Considered altogether , the three criteria we advocate produce a suppression of background γ triplets at the level of 60 % without affecting the magnitude of the ρ^0/ω signals. In particular, the π^0 peak is totally removed. A part of the background is due to non–removed split–offs, however another part is physics mainly associated with one lost photon.

The events surviving all the previous cuts give entries in downmost figure 12. Keeping only

those events from there satisfying also energy–momentum conservation (±60 MeV), we get the histogram in figure 13. This mimics the effect of using CBDROP. Here, some $\rho/\omega \rightarrow \gamma\gamma\gamma$ are lost, but the background is reduced by another factor of 3.

8 Conclusion

From this study, we conclude that, in order to remove hadronic – and to some extent – electromagnetic split–offs, an efficient way is to require the following set of conditions :

i/ The clusters matching the charged tracks have to be considered globally. These clusters are constructed using the taxiblock algorithm. Practically, it turns to remove the matched PEDs ; for unmatched PEDs, there is presently a flag in the TTKS bank provided by the global tracking (word 53). If the flag is zero, it means that the corresponding PED does not belong to a cluster matching a charged track. It can be used safely provided the following conditions are also fulfilled.

ii/ The central crystal energy of each unmatched PED has to be larger than 8 MeV (13 MeV is more relevant in connection with Monte Carlo simulations). This parameter is presently given as word 13 in the TTKS bank for PEDs.

iii/ Each unmatched PED has to carry a value for E1/E9 smaller than 0.96. This parameter can presently be found as word 33 in the TTKS bank.

The first two conditions push the hadronic split–off probability to about 15 % per charged track. The last condition reduces further this probability to about 12 % and moreover helps to remove also electromagnetic split–offs.

These criteria should be used together with criteria better adapted to the removal of electromagnetic split–offs like Dolby–C or SMART.

The efficiency of these criteria has been shown on 2–prong events with three unmatched PEDs ; they allow here to remove half of the background without noticeably affecting the single physics signal in this channel ($\rho^0/\omega \rightarrow \pi^0/\eta\ \gamma$).

References

[1] J.E. Salk, Smart – Split–off Recognition in Pure Neutral Events, CB Note 182, oct. 1991.

[2] N.P. Hessey, Split–off Recognition with Dolby–C, CB Note 182, aug. 1992.

[3] J.E. Salk, Spit-off Recognition with SMART and Dolby–C (Performance Study), CB note 216, sept. 1992.

[4] M. Burchell, Hadronic Split–offs, CB note 201, jul 1992.

[5] C. Meyer, User Guide for CBDROP, A charge Split–off Supression Package, CB note 191, june 1992.

[6] A.J. Noble, A study of Hadronic Interactions in CBGEANT, FLUKA vs GEISHA, CB note 258, july 1994.

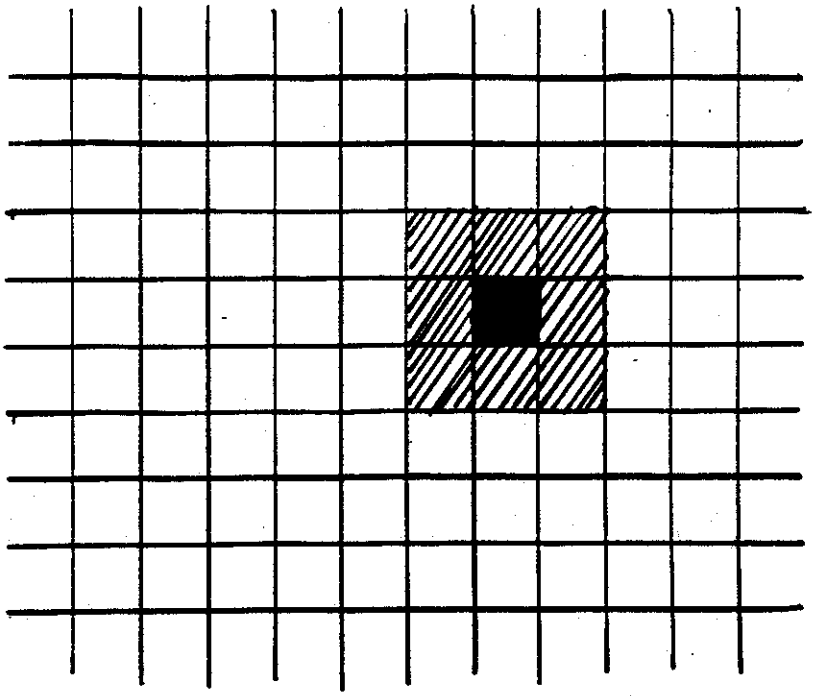

Figure 1 : The usual neiborhood (shadded crystals) of a crystal (shown in black). The Crystal Barrel Calorimeter is figured by a lattice. If the crystal shown in black is fired (*i.e.* above threshold), one looks among its eight neighbors (shadded squares), which crystals are also fired ; any fired crystal among them is added to the cluster and one looks to its fired neighbors as just described.

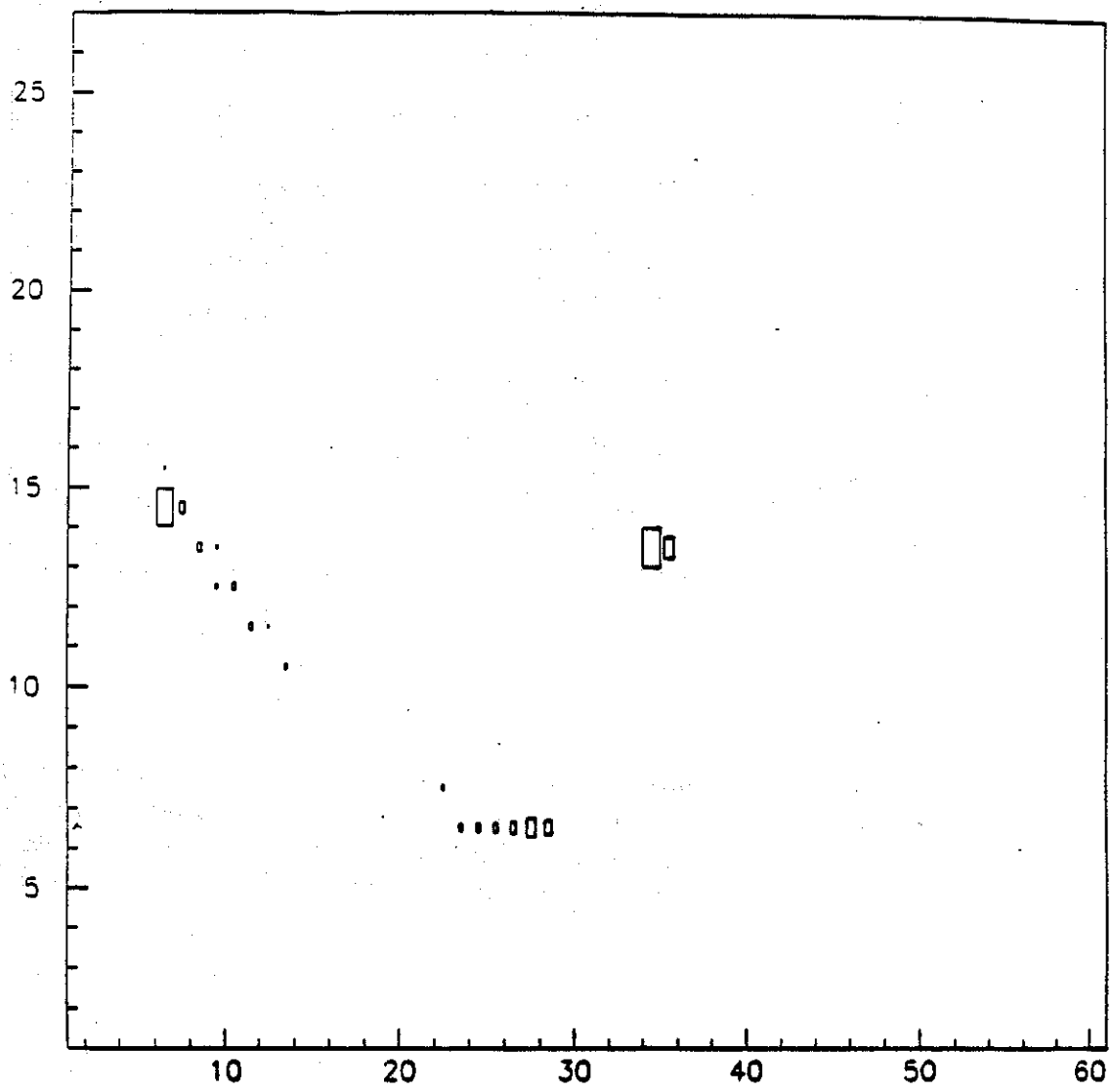

Figure 2 : A collinear event. Along the vertical axis, the θ coordinate, along the horizontal axis the ϕ coordinate (see text). The two clusters matching the charged tracks are those having the largest θ coordinates. The split–off cluster is downmost and cannot be attributed unambiguously to one of the parent (matched) clusters.

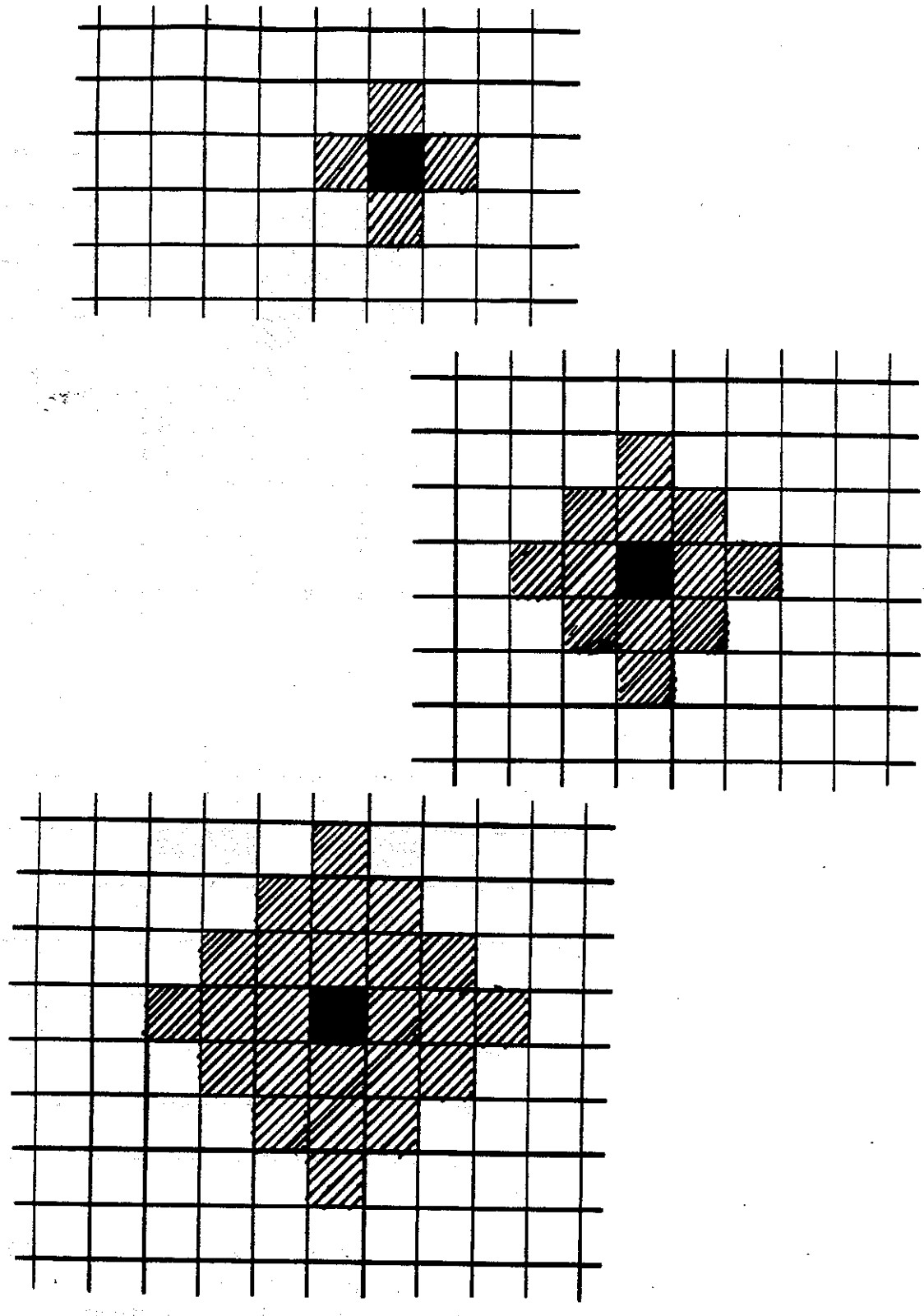

Figure 3 : Alternative definitions of crystal neighborhoods to the usual one (see figure 1). Upmost figure shows the neighborhood of the black crystal when using a taxiblock distance $k = 1$; middle figure shows the neighborhood of a given crystal if $k = 2$, while the dowmost figure illustrates the case $k = 3$.

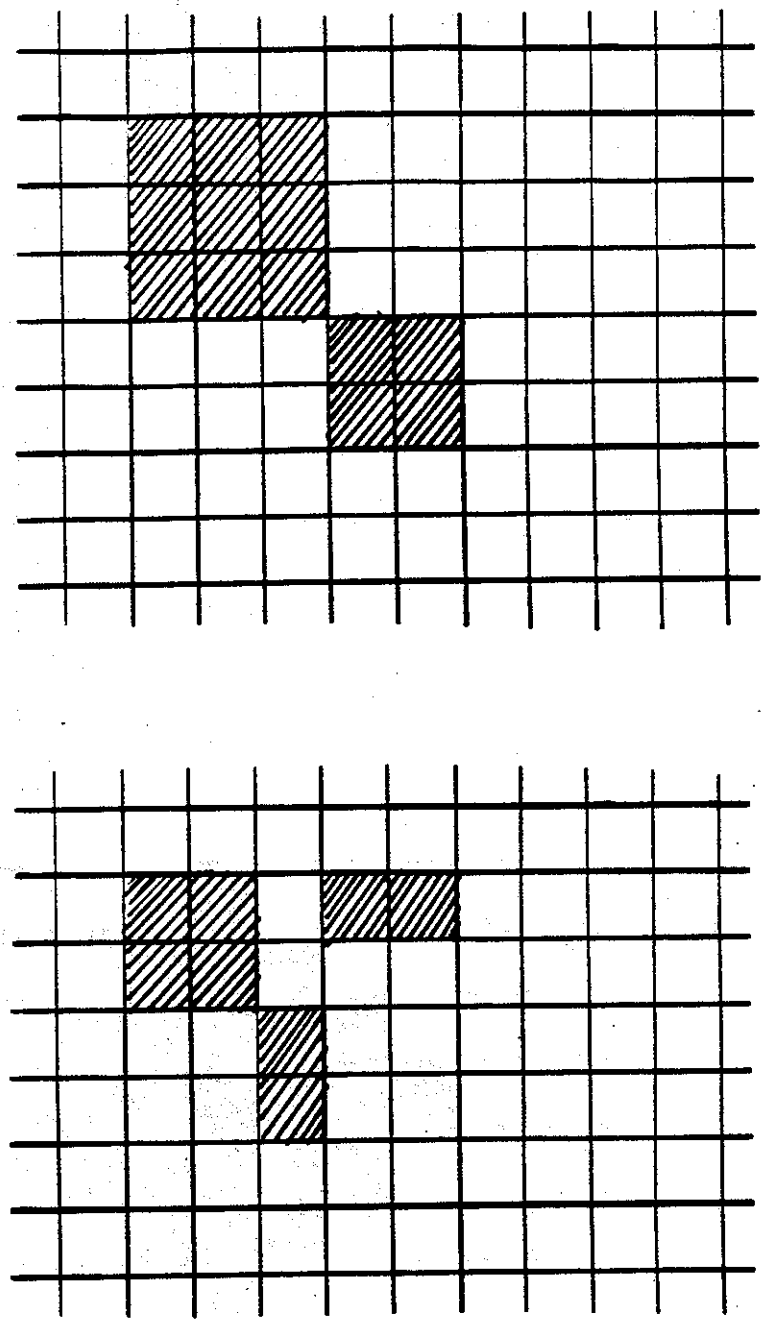

Figure 4 : Clusters of crystals. In the upper figure, the standard neighborhood algorithm finds one cluster, as the taxiblock algorithm with $k = 2$ or $k = 3$, while using $k = 1$ the taxiblock algorithm finds two clusters. Downmost figure : the standard algorithm finds two clusters, while the taxiblock algorithm with $k = 2$ or $k = 3$ finds one cluster.

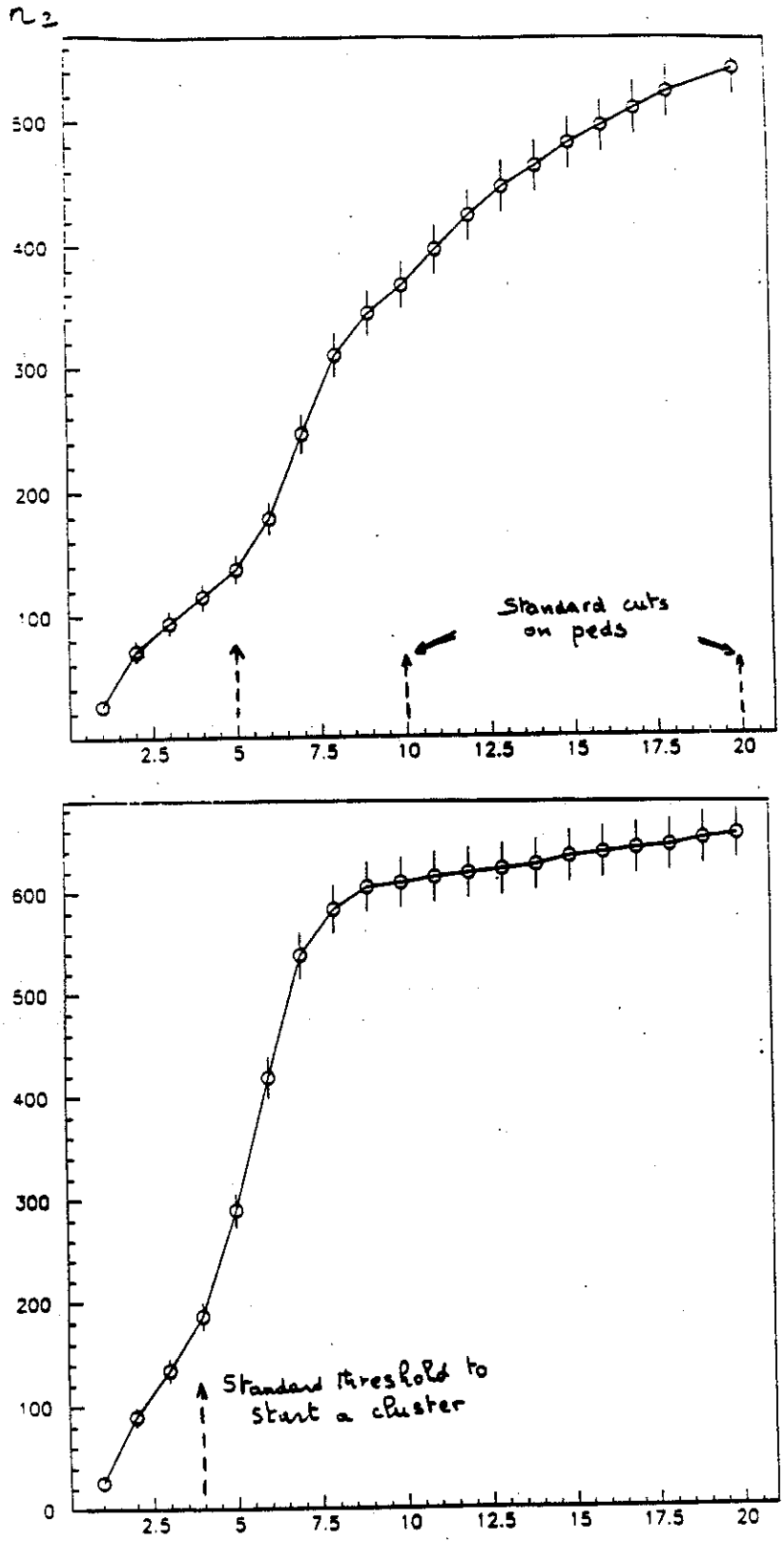

Figure 5 : Number of 2–cluster events in a sample of collinear events (real data) as a function of threshold energy values for different parameters. In the upmost figure, the parameter is the cluster energy (ECLUBC) and a cluster is counted if its energy is above the threshold value given in abscissa. In the downmost figure, the relevant parameter is the central crystal energy (EXTSBC) of the clusters.

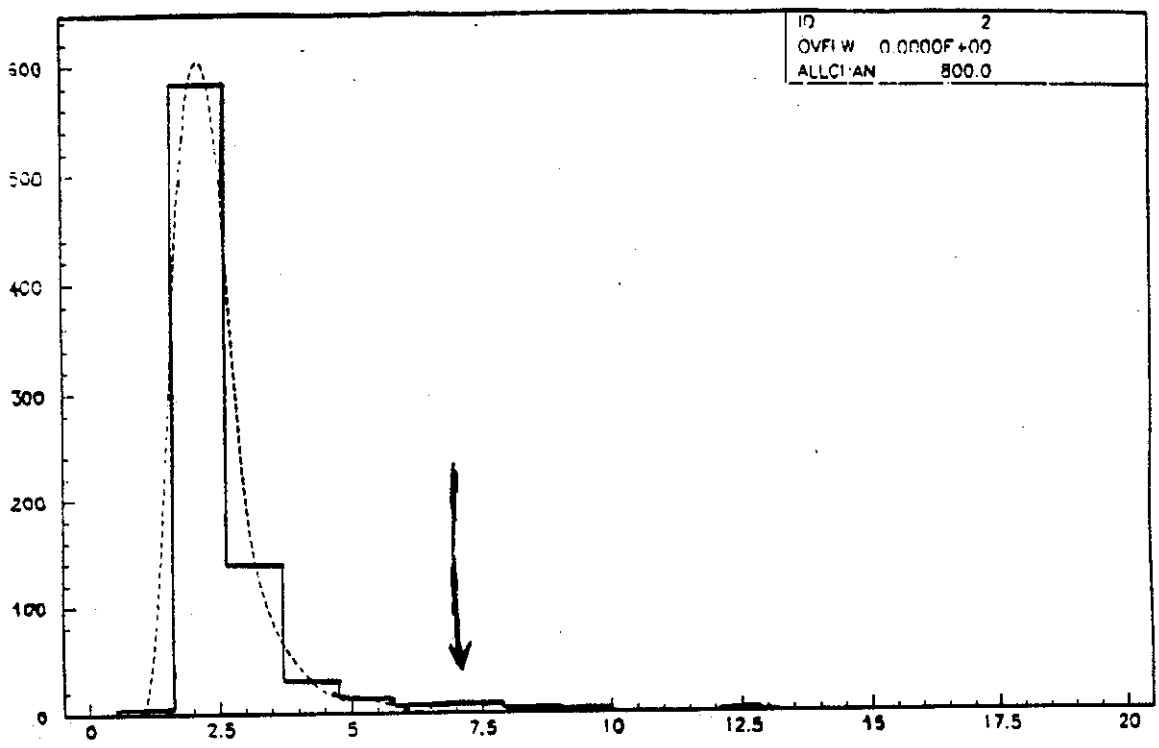

Figure 6 : Distribution of the number of clusters in a sample of collinear events (real data). A cluster is counted if its central crystal energy is above 8 MeV.

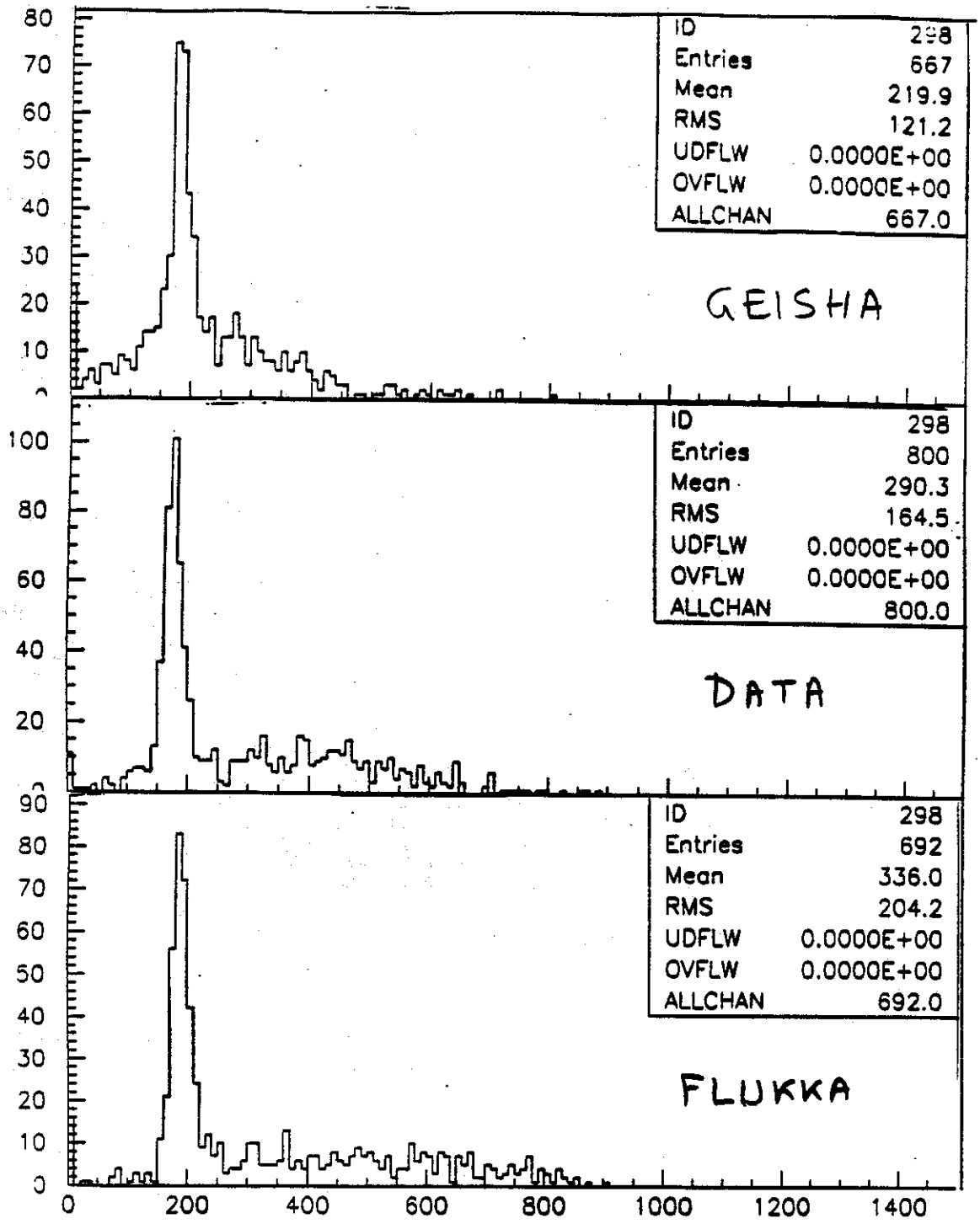

Figure 7 : Energy in MeV of the matched clusters in samples of collinear events (pions). Upmost figure is simulation data generated using GEISHA, middle figure is obtained from real data and downmost figure is obtained from simulation data generated using FLUKA. The minimum ionizing peak is always well described, but the reinteraction bump is shifted towards too low energy with GEISHA.

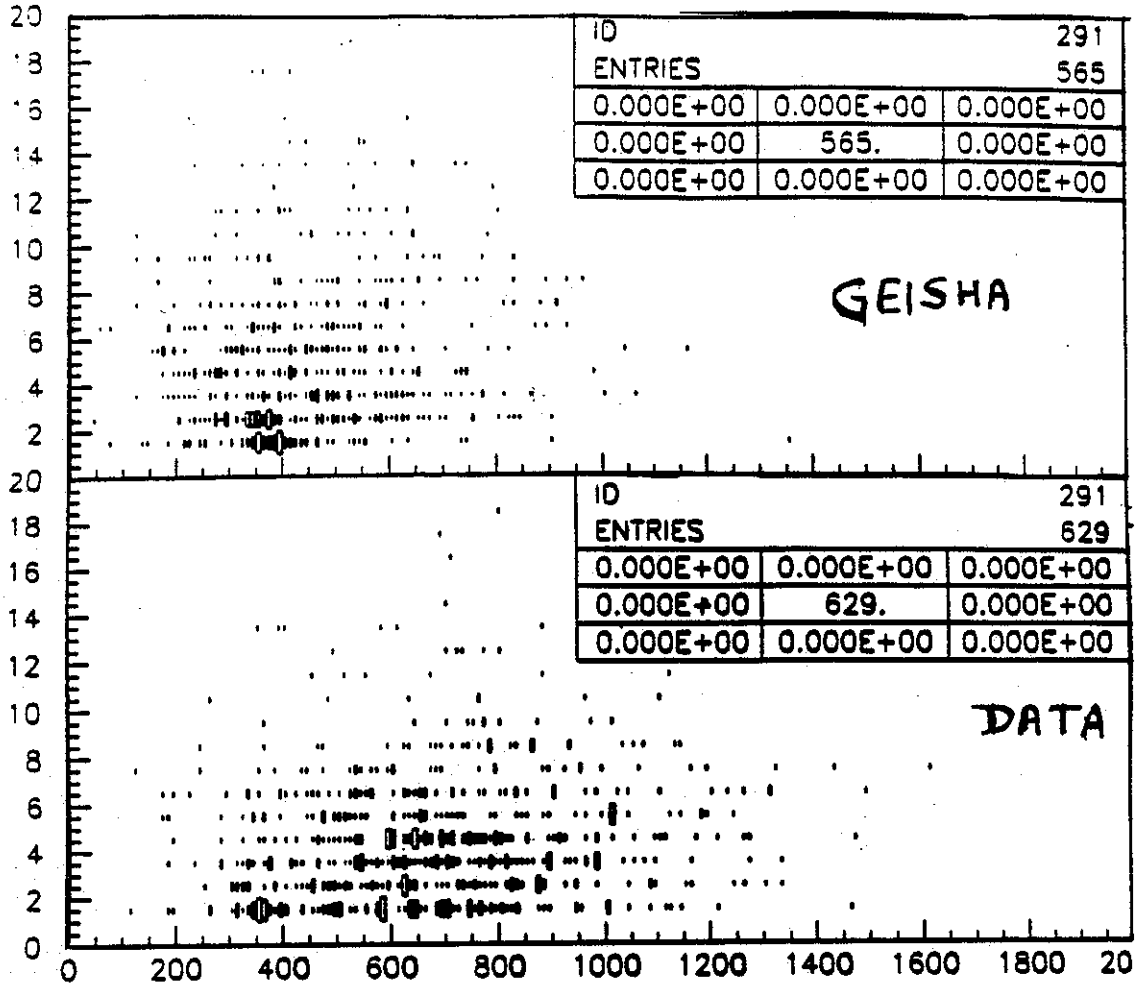

Figure 8 : Number of split–offs in collinear events as a function of the the total energy carried by the two matched clusters. Upper figure is for simulation data obtained using GEISHA, while downmost figure is for real data.

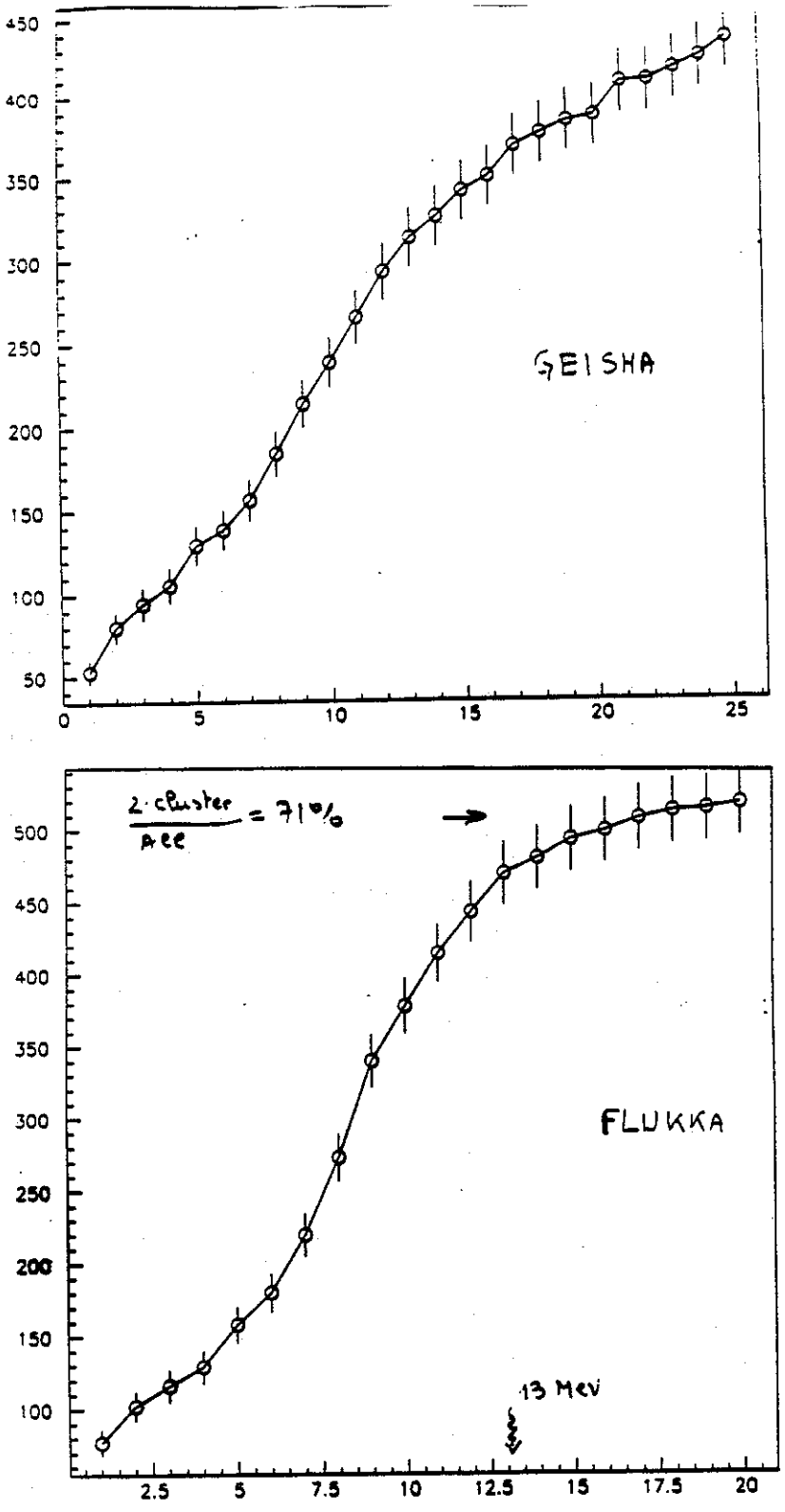

Figure 9 : Number of 2–cluster events in a sample of collinear events (simulation data) as a function of the threshold energy value for the central crystal energy (EXTSBC). The sample obtained with GEISHA does not exhibit any stable regime, while the sample generated using FLUKA does as the experimental data (see figure 5). However the stable regime begins around 13 MeV instead of 8 MeV (real data).

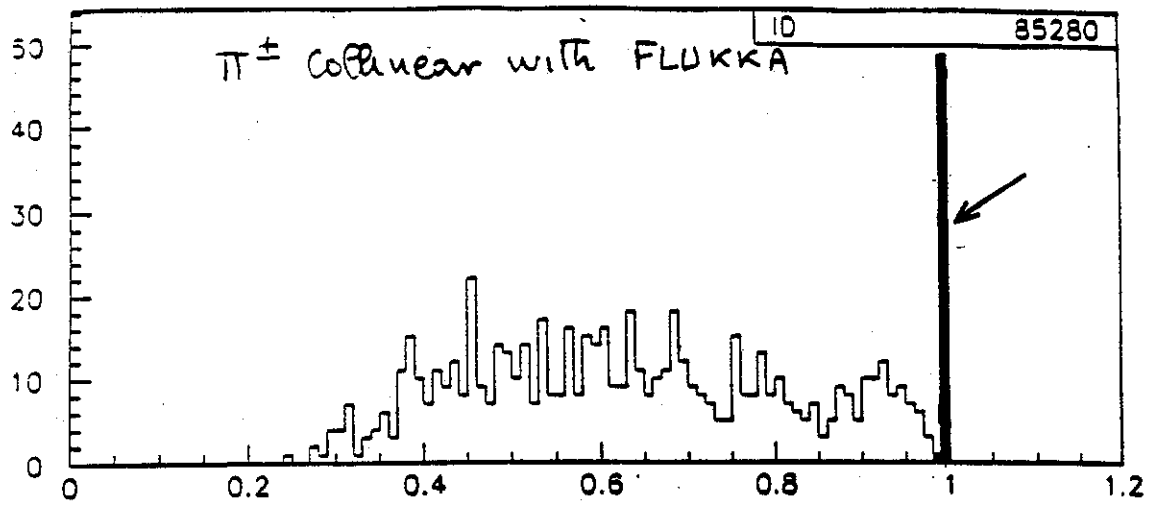

Figure 10 : Distribution of E1/E9 for PEDs in collinear events generated with FLUKA. The peak above 0.96 shows split–offs of one crystal size.

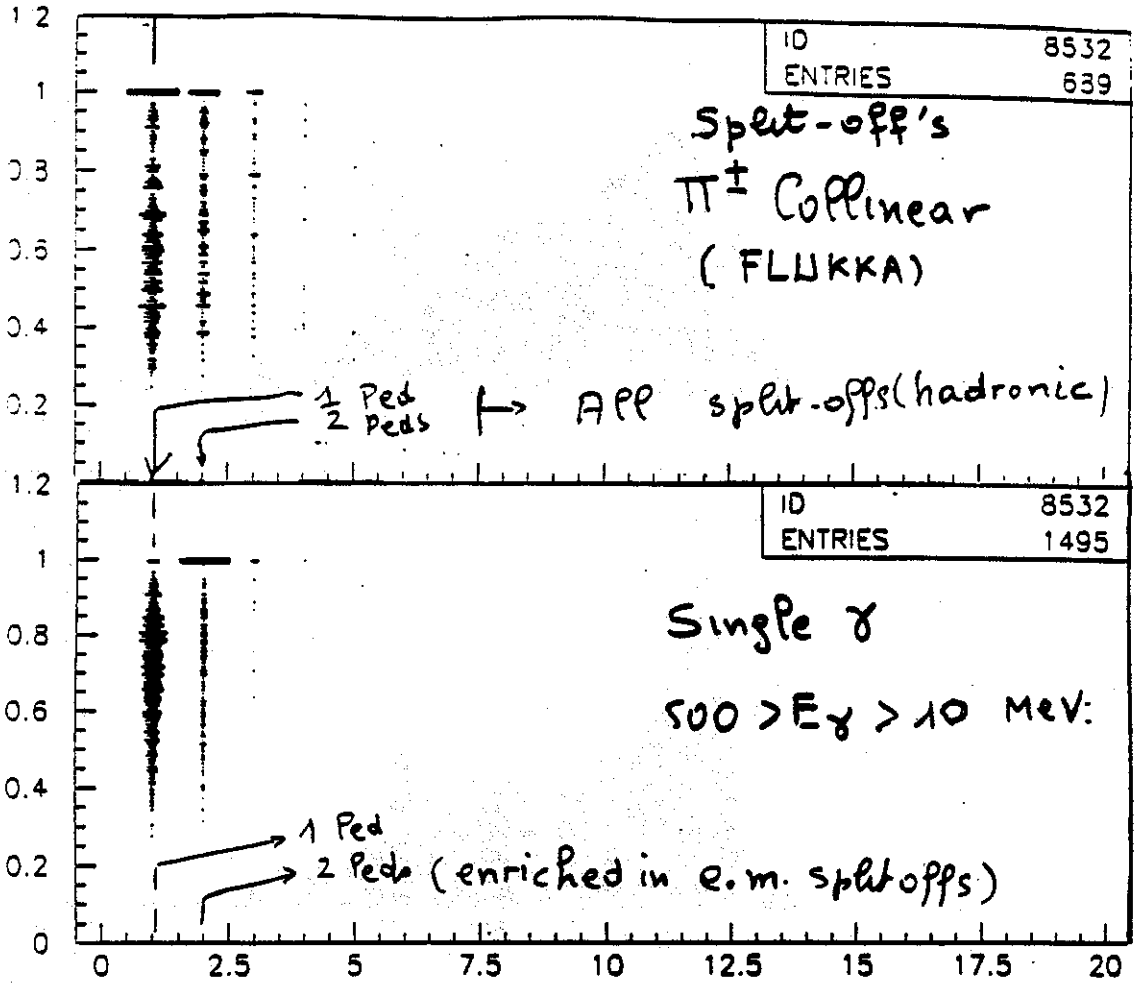

Figure 11 : For simulation events. Upmost figure shows the PED distribution of E1/E9 for split–offs in collinear events ; a large fraction of these split–off PEDs carries values of E1/E9 above 0.96. Dowmost figure shows the total number of PEDs for simulated single photons carrying an energy between 10 MeV and 500 MeV ; the number of 2–PED events is highly enriched in PEDs with E1/E9 $\geq$ 0.96. The presence of PEDs with E1/E9 $\geq$ 0.96 indicates split–offs with a good probability.

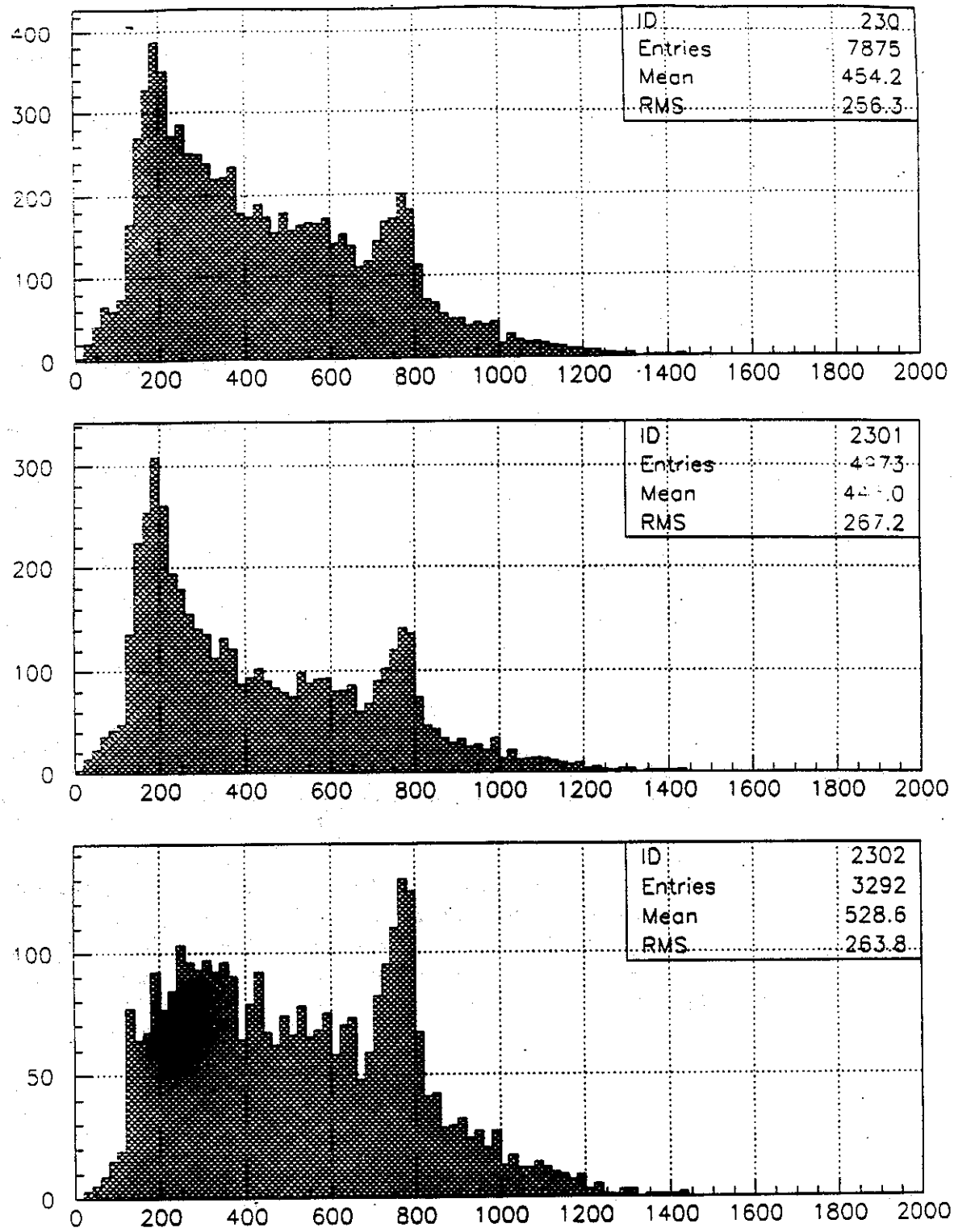

Figure 12 : Invariant three photon mass distribution in the final state $\pi^+\pi^-\gamma\gamma\gamma$. Upmost figure, after using Dolby–C to remove electromagnetic split–offs. Middle figure is obtained by removing in addition events where one among the three photons is found inside one of the two hadronic clusters. Dowmost figure is obtained from the previous one after removing also PEDs which have E1/E9 $\geq$ 0.96 or having a central crystal energy below 8 MeV. The peak at 200 MeV is due to a π^0 with a small energy split–off, the peak around 800 MeV is due to $\rho^0/\omega \rightarrow \gamma\gamma\gamma$. The procedure removes the peak at 200 MeV and leaves unaffected the peak at 800 MeV.

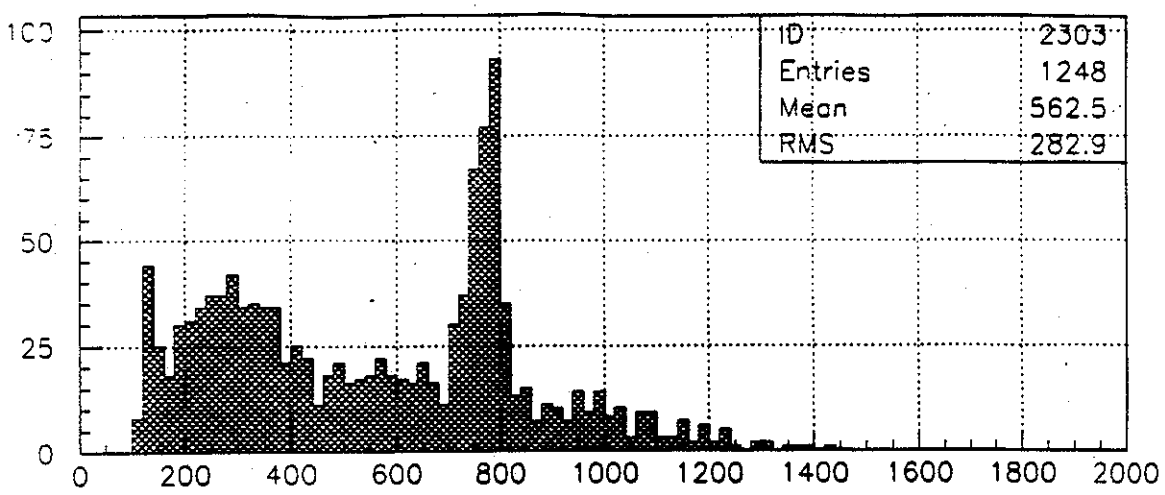

Figure 13 : Same data as in the downmost figure 12 by asking in addition the final state invariant mass to be that of $p\overline{p}$ in a window of ± 60 MeV.